

Quantum phase transition in the spin boson model

S. Florens, D. Venturelli and R. Narayanan

Abstract In this paper we give a general introduction to quantum critical phenomena, which we practically illustrate by a detailed study of the low energy properties of the spin boson model (SBM), describing the dynamics of a spin $1/2$ impurity (or more generically a two-level system) coupled to a bath of independent harmonic oscillators. We show that the behavior of the model is very sensitive to the bath spectrum, in particular how the properties of the quantum critical point in the SBM are affected by the functional form of the bath Density of States (DoS). To this effect, we review the renormalization group (RG) treatment of the SBM for various bath DoS, based on an unconventional Majorana representation of the spin $1/2$ degree of freedom. We also discuss the derivation of Shiba's relation for the sub-ohmic SBM, and explicitly derive an effective action vindicating the quantum to classical mapping.

1 Introduction

Quantum Phase Transitions (QPT) have recently become a widespread topic in the realm of modern condensed matter physics. QPT are phase transformations that occur at the absolute zero of temperature and are triggered by varying a temperature independent control parameter like pressure, doping concentration or magnetic field. There are various examples of systems showing quantum critical behavior, which include the anti-ferromagnetic transition in heavy fermion material like $\text{CeCu}_{6-x}\text{Au}_x$, that is brought about by changing the Au doping [11]. Another prototypical exam-

S. Florens
Institut Néel, CNRS and UJF, 38042 Grenoble, France

D. Venturelli
Institut Néel, CNRS and UJF, 38042 Grenoble, France

R. Narayanan
Department of Physics, Indian Institute of Technology, Chennai-600036, India

ple of a system exhibiting quantum critical behavior is the Quantum Hall Effect, wherein a two-dimensional electron gas is tuned, via an externally applied magnetic field, through a quantum critical point (QCP) that intervenes between two quantized Hall plateaux. Other examples of QPT include the ferromagnetic transition in metallic magnets as a function of applied pressure, and the superconducting transition in thin films.

Since there are such a wide range of experimentally accessible systems that show quantum critical behavior, it is imperative that we understand QPT at a fundamental level. We shall here endeavor to do just so by giving an introductory account of this fascinating phenomenon. As a striking illustration, we will be comparing and contrasting QPT with the case of more usual thermal (classical) phase transitions (as will be seen later on, thermal phase transitions are also referred to as classical transition, since quantum fluctuations become unimportant in their vicinity). Let us first begin by discussing the ferromagnetic transition, in order to better illustrate the rich phenomenology of phase transitions (both classical and quantum). The route that we take here to understand the fundamentals of QPTs is as follows: We shall first review the basic phenomenology of classical (thermal) phase transitions. Then, we shall illustrate via heuristic arguments how quantum fluctuations can be disregarded in the vicinity of a thermal phase transition. These arguments also provide clues to the domain in the phase diagram where one expects quantum fluctuations to dominate. Also, we shall briefly discuss the question of observability of QPTs. Finally, we shall end with a discussion of the so called quantum to classical mapping.

Let us first start with classical (thermal) phase transitions. As a physical system, say a ferromagnet, approaches its ordering, there is a length scale called the correlation length, ξ that diverges in a power-law fashion when one comes closer to the critical point, $\xi \sim |t|^{-\nu}$, so that the system becomes progressively self-similar. Here, t is dimensionless parameter characterizing the distance to criticality, $t = \frac{T-T_c}{T_c}$ (for a thermal transition), and T_c is the critical temperature where the phase transformation occurs. Now, the above divergence of the correlation length encapsulates the information that the fluctuations of the order-parameter (say the magnetization) become spatially long-ranged as the system approaches the critical point. Analogous to ξ one can define a time scale ξ_τ , that also diverges as a power law as one approaches a second order transition. Thus, we have:

$$\xi_\tau = \xi^z = |t|^{-\nu z} \quad (1)$$

The quantity z that controls the divergence of ξ_τ is the so called dynamical exponent. Now, associated with this time scale we can define a frequency scale $\omega_c \propto 1/\xi_\tau$, and through it a corresponding energy $\hbar\omega_c$, which encodes information pertaining to the energy scale related with order-parameter fluctuations. This quantity $\hbar\omega_c$ competes with $k_B T_c$, the typical energy associated to thermal fluctuations. Now, the question of importance of quantum fluctuations can be re-cast into a query of which among these two energy scales prevails. Since $\omega_c \rightarrow 0$ as one approaches the critical point, the energy scale of thermal fluctuations (for any non-zero T_c) always dominates over the scale $\hbar\omega_c$. In other words for a transition that happens at a finite temperature,

$\hbar\omega_c \ll k_B T_c$. Thus, it can be argued that asymptotically close to a finite temperature transition, it is the thermal fluctuations that are the driving mechanism. This irrelevance of quantum fluctuations near a thermal phase transition is the reason to why they are given the moniker “classical phase transition”.

Now, from our discussion in the previous paragraph it is but obvious that if the transition were to occur at $T = 0$ (tuned by a non-thermal parameter like doping or pressure), then the fluctuations that will drive the transition will be wholly quantum mechanical in origin. It is obvious that one then needs to apply ideas from quantum statistical mechanics to understand QPT, as pioneered by Hertz in a seminal paper [7] to tackle the problem of quantum criticality in itinerant magnetic systems. By using this case of the quantum magnet as a test-bed example, Hertz [7] showed that any generic d dimensional quantum system can be mapped onto an equivalent $d + z$ dimensional classical model. This statement is referred to as the quantum to classical mapping and is of fundamental importance in the field of QPTs. By using the quantum to classical mapping one can show that the critical behavior of the quantum model is equivalent to that of a classical model but in z higher dimensions. Although this mapping is believed to be robust for insulating magnets, it was however later shown [1] that Hertz’s conclusions were erroneous for a large class of itinerant QPT. This break-down in fact occurs due to the presence of soft modes in the systems (e.g. the particle-hole excitations in itinerant magnets) other than the order-parameter modes. The presence of these modes induces an effective long-ranged interaction between the order-parameter modes, thereby altering the critical behavior [1], as compared to Hertz’s original results.

Since QPT occur at zero temperature, it was initially thought that the study of these phase transitions was a mere academic exercise. However, it was soon realized that the presence of a zero-temperature critical point (practically inaccessible) can actually influence the behavior of the system at *finite* temperatures. In other words, at any finite temperature, the critical singularities associated with the QCP are cut by the temperature, so that one observes non-trivial temperature dependence of various observables in a so-called quantum critical regime. The calculation of the quantum critical regime for various models is well beyond the scope of this work. However the interested reader is directed towards the following papers investigating the effect of non-zero temperatures on QPT in magnetic systems [20, 23]. Also, one will refer to Sec. 2.2 for a brief description of the quantum critical regime in the spin boson model (SBM), the specific model of interest in this manuscript.

Thus, from the discussion of previous paragraphs, it is obvious that QPT are an extremely interesting physical phenomenon to study. As alluded to before, in this manuscript we choose to study a specific toy model example, namely the QPT encountered in the spin boson model (SBM), a variant of Caldeira-Leggett type models [9], wherein a quantum particle is subjected to an external dissipative environment. In the case of the SBM, this quantum “particle” is essentially a two-level system, such as a spin $1/2$ impurity. While there have been many studies on dissipative quantum models that focused on the effect of decoherence on intermediate time scales, their behavior in the long time limit in the presence of quantum critical points remain relatively un-explored. However, the study of such regimes is extremely important

as anomalous low energy properties emerge due to quantum critical modes. In other words, due to the presence of a QCP, the SBM can display non-trivial dynamics at very long times.

As a more general remark, we note that this model can also be used to study quantum criticality at the level of a single spin $\frac{1}{2}$ impurity embedded in a correlated system such as Mott insulators [3, 13, 18], or magnetic metals [8, 10]). It also appears as an effective theory for bulk materials themselves (e.g. in quantum spin glasses [16], heavy fermion compounds [15, 17]), via the framework of DMFT.

The SBM is introduced in Sec. 2. The various phases of the SBM and the possibility of a QPT between them is discussed in Sec. 2.2. In Sec. 3, we re-write the SBM by using a Majorana fermion representation for the impurity spins. Sec. 4 is devoted to the derivation of the RG equations by using the Majorana representation presented in Sec. 3. In Sec. 5, we look at the consequences of the flow equation derived in Sec. 3. Sec. 6 is dedicated to the quantum/classical mapping of the SBM to the long-ranged Ising model. Sec. 7 is concerned with the development of a special identity in the SBM model that is used in Sec. 8 to derive the so-called Shiba's relation in the case of the sub-ohmic spin boson model. Sec. 9 is dedicated to a discussion on the status of the quantum to classical mapping in the SBM, that we use as a conclusion and future outlook regarding quantum phase transitions in dissipative models.

2 The Spin Boson Model

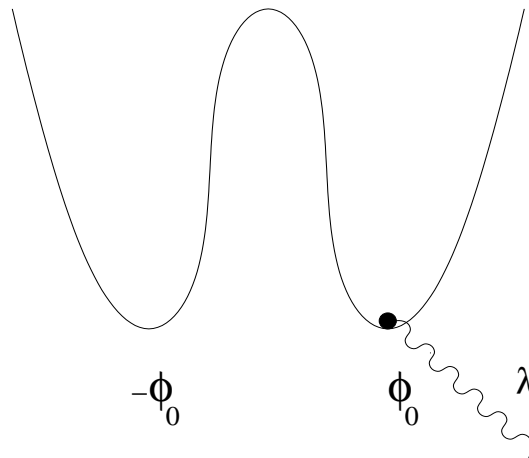


Fig. 1 Fig. 1 is a pictorial sketch of the SBM. It represents a two level system (e.g. a particle in two potential minima $\pm\phi_0$, or a spin $1/2$ impurity, coupled to a bath of harmonic oscillators (such as phonons, nuclear spins,...) via a coupling constant λ (wavy line in this figure).

As stated earlier, the SBM describes the effect of an external dissipative environment on the quantum mechanical evolution of a two-level system. We will introduce in Sec. 2.1 the general properties of the SBM, and present in Sec. 2.2 its possible phase diagram, obtained on heuristic grounds via an analysis of the various limiting cases.

2.1 The Model

The SBM involves a single spin $\frac{1}{2}$ impurity \mathbf{S} , interacting with a set of bosonic bath variables, a_i , and a_i^\dagger (in second quantization). The interaction between the bath's oscillator displacement and the spin is controlled via a coupling constant λ . Thus, the SBM Hamiltonian has the general functional form:

$$H = -\Delta S^x + \varepsilon S^z + \lambda S^z \sum_i (a_i^\dagger + a_i) + \sum_i \omega_i a_i^\dagger a_i. \quad (2)$$

Here, in Eq. 2, Δ and ε are the transverse and longitudinal magnetic fields respectively, applied to the quantum spin. A physical sketch for such a SBM, wherein a two-level impurity (when the bias field ε is set to zero) is connected to an external environment, is depicted in Fig. 1. All that remains to completely specify the model is to endow the bosonic degrees of freedom with a spectrum. This bosonic density of states (DoS) is taken here to be continuous and power-law like, and conforms to the functional form:

$$\rho(\omega) \equiv \sum_i \delta(\omega - \omega_i) = \frac{(s+1)\omega^s}{\Lambda^{1+s}} \theta(\omega) \theta(\Lambda - \omega). \quad (3)$$

Here, in Eq. 3, Λ is a high-energy cutoff. When the exponent s is such that $0 < s < 1$, then the model is said to be in the sub-ohmic regime, the case $s = 1$ is referred to as ohmic, while the case $s > 1$ is called super-ohmic. In fact, as will be seen in the course of this paper, the quantum critical behavior of the SBM is crucially dependent on the exponent s controlling the behavior of the bath spectrum.

It is also convenient to define a new bosonic variable corresponding to the ‘‘local’’ displacement:

$$\phi \equiv \sum_i (a_i + a_i^\dagger), \quad (4)$$

which has an associated DoS given by,

$$\rho_\phi(\omega) = -\frac{(s+1)|\omega|^s}{\Lambda^{1+s}} \text{sgn}(\omega) \theta(\Lambda^2 - \omega^2). \quad (5)$$

To make comparison with existing literature, one can alternatively characterize the bath by means of a spectral function:

$$J(\omega) \equiv \sum_i \pi \lambda^2 \delta(\omega - \omega_i) = 2\pi \alpha \omega^s \Lambda^{1-s} \theta(\omega) \theta(\Lambda - \omega). \quad (6)$$

Here α is the non-dimensional dissipation strength defined as $\alpha = (s+1) \frac{\lambda^2}{\Lambda^2}$.

2.2 The Phases of the SBM

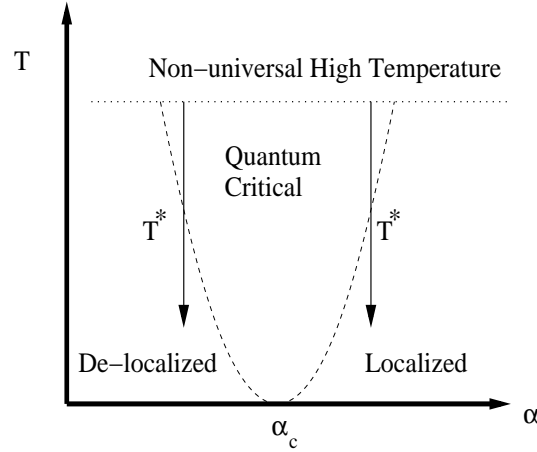


Fig. 2 Fig. 2 shows the generic phase diagram of the SBM model. Here, a quantum critical point α_c separates localized and delocalized phases, from which a quantum critical region emerges at finite temperature. The scale T^* is the cross-over temperature below which various physical observables revert from quantum critical behavior to those associated with the localized or the delocalized phase.

As promised in Sec. 2, we will study here the possible phase diagram of the SBM by looking at situations where either one of the two parameters λ or Δ dominates. For instance, let us first consider the case where the dissipative coupling λ is set to zero. The SBM then becomes equivalent to the case of an isolated spin in a transverse magnetic field. It is well known that such a system displays Rabi oscillations. That is, if one were to start with an initial state pointing “up” along the z direction, then the transverse field Δ periodically drives the system between up and down configurations. This limiting case $\lambda = 0$ is in fact adiabatically related to a whole phase at non-zero λ , dubbed for obvious reasons the delocalized phase, where coherent spin oscillations are expected to occur (at least for small enough λ). We note that the average $\langle S^x \rangle$ is always non-zero as long as the transverse field Δ is finite, and thus cannot play the role of an order parameter. However, we can pursue a magnetic analogy by noting that the longitudinal spin average $\langle S^z \rangle$ is identically zero in the delocalized phase, so that we can really relate this portion of the phase diagram to a

ground state with zero magnetization. In fact in the alternative regime, i.e. when the dissipation λ dominates over the transverse field Δ , the ground state becomes doubly degenerate, as can be checked on the trivial limiting case $\Delta = 0$, where the z spin component is clearly conserved within the Hamiltonian (3). A simple physical picture emerges, with the system localizing in one of the two minima at $\pm\phi_0$, see Fig. 1. Assuming adiabaticity by switching on the transverse field, we arrive to the so-called localized phase, wherein the spontaneous magnetization $\langle S^z \rangle \sim \langle \phi \rangle \equiv M \neq 0$. Now, so far by using heuristic arguments, we have shown that the SBM allows for the existence of a de-localized phase, with $\langle \phi \rangle = 0$, and a localized phase, with $\langle \phi \rangle \neq 0$. Thus, it is quite plausible that a second-order phase transition takes place between the two phases. As we shall see explicitly in Sec. 5, there is indeed a second order quantum localization/delocalization transition for all $0 < s \leq 1$.

The generic phase diagram for the SBM is shown in Fig. 2, where a $T = 0$ phase transition, separating localized and delocalized phases, takes place at a critical value α_c of the adimensional dissipation strength. The interesting quantum critical regime emerges above the critical point at finite temperature, where anomalous behavior of all physical quantities is expected. For instance, the longitudinal spin susceptibility in the quantum critical regime obeys the behavior $\chi_z(T) \sim 1/T^s$, as opposed to the conventional $1/T$ Curie-law expected for the whole localized phase. This anomalous power-law behavior is a direct signature of the QCP at α_c , and will be demonstrated in the following sections. We note that for the ohmic $s = 1$ case, the conventional treatment for studying the QPT is to map the SBM into an anisotropic Kondo model (AKM), and use previous knowledge on the scaling properties of this well-known Hamiltonian. However, in this paper, we shall follow a less well-trodden path, namely, performing a renormalization group (RG) calculation directly within the SBM, using a spin representation in terms of Majorana fermions (see Sec. 3 for further details). This formalism has the advantage that it can be easily adapted to perform calculations in the sub-ohmic limit, i.e. ($0 < s < 1$), see Sec. 4.

3 The SBM using the Majorana representation

In Sec. 4 we aim to derive the RG equations for the SBM, based on a perturbative analysis around the localized limit, i.e. $\Delta = 0$. A technical difficulty on this path comes from the fact that the quantum spin $\frac{1}{2}$ impurity does not follow either bosonic or fermionic commutation relations. Thus, standard calculations based on Wick's theorem cannot be invoked. One of the many ways to avoid this problem is to map the spin- $\frac{1}{2}$ operator onto fermionic degrees of freedom, which can be done in particular using so-called Majorana fermions. The use of this mapping to condensed matter is relatively recent and for a more detailed explanation the readers are referred to the following references, Refs. [22, 21].

The mapping between the spin $\frac{1}{2}$ impurity and the Majorana fermions obey the following correspondence principle:

$$\vec{S} = -\frac{i}{2} \vec{\eta} \times \vec{\eta} \quad (7)$$

Here, in Eq. 7 the η fields represent a triplet of Majorana (real) fermions $\eta \equiv (\eta_1, \eta_2, \eta_3)$, that satisfy the following anticommutation relations $\{\eta_i, \eta_j\} = \delta_{ij}$. Now, in addition to these Majoranas defined above, one can construct another fermionic field, $\Phi = 2i\eta_1\eta_2\eta_3$, that commutes with the Hamiltonian, and constitutes hence a conserved quantity, with the constraint $\Phi^2 = \frac{1}{2}$. A very useful relation for describing the spin dynamics is given by the correspondence (see [21]):

$$\vec{\eta} = 2\Phi \vec{S} \quad (8)$$

Now, in terms of the Majorana fermions (see Eq. 7), and after the redefinitions $\{S_x \rightarrow S_3, S_y \rightarrow S_2, S_z \rightarrow S_1\}$ which amounts to a $\pi/2$ rotation around the y direction, the Hamiltonian of the SBM can be expressed as

$$H = -i\frac{\Delta}{2} (\eta_1\eta_2 - \eta_2\eta_1) + H_B - i\lambda\phi\eta_2\eta_3 \quad (9)$$

Now in what follows, we will use Eq. 9 to perform the perturbative RG analysis. Before we go on to do so, a word of caution regarding the fermionic mapping is in order: Any mapping of the spin $\frac{1}{2}$ impurity to fermionic operators tends to enlarge the dimensionality of the Hilbert space. How such an enlargement is obviated in the case of the Majorana representation is technical matter that goes well beyond the scope of this manuscript, and the reader is directed to Refs. [21, 22] for further details.

4 Perturbative renormalization group in the localized regime

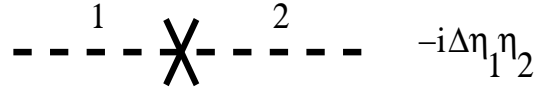


Fig. 3 Pictorial representation of the Δ vertex.

In this section, we will perform a perturbative RG treatment starting from the localized phase, i.e. from the limit in which $\Delta = 0$. Our plan of action to derive the RG equations is as follows: We initially start with a model of free spin ($\Delta = 0$, $\alpha = 0$), and then perform a perturbative analysis in both Δ and α , leading to renormalizations of the dissipation α and the transverse field Δ , which depend explicitly on a generic cut-off scale Λ . Following the philosophy of the RG, one aim to compute the renormalized parameters at a lower cut-off scale, Λ' , leading to so-called flow equations.

The key ingredient in developing the perturbation theory are the free Majorana fermion propagator G_η^{free} , as well as the Δ vertex shown in Fig. 3, and the λ vertex (first diagram appearing in Fig. 4). The free fermion propagator in Matsubara frequency $\omega_n = (2n+1)\pi T$ at finite temperature T reads $G_\eta^{\text{free}}(i\omega_n) = 1/i\omega_n$. One can then first construct the vertex function Γ_α related to the dissipative coupling λ , shown in Fig. 4. The functional form of the vertex function can easily be deduced

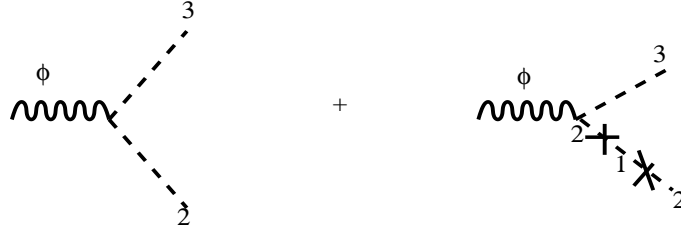


Fig. 4 Lowest order diagrams involved in the renormalization of the dissipative term λ .

to be

$$\Gamma_\alpha(\omega, \Lambda) = \frac{\lambda}{\Lambda} + \frac{\lambda}{\Lambda} \Delta^2 G_\eta^{\text{free}}(\omega)^2 \quad (10)$$

Here, once again Λ is cut-off scale, set e.g. by temperature or the bandwidth of the bosonic modes, and ω is a frequency. The above equation can be effectively re-written in terms of an adimensional transverse field $h = 2\Delta/\Lambda$, so that the renormalized dissipation reads:

$$\Gamma(\omega, \Lambda) = \frac{\lambda}{\Lambda} \left[1 - \frac{h^2}{4} \exp\left(2 \ln \frac{\Lambda}{\omega}\right) \right] \quad (11)$$

Now, as stated in the introductory part of this section, we re-scale the cut-off Λ to $\Lambda' = \Lambda - d\Lambda$. Under such a re-scaling the vertex function can be re-written as:

$$\Gamma(\omega, \Lambda') = \frac{\lambda}{\Lambda'} \left(1 + \frac{d\Lambda}{\Lambda} \right) \left[1 - \frac{h^2}{4} \exp\left(2 \ln \frac{\Lambda}{\omega}\right) + \frac{h^2}{2} \frac{d\Lambda}{\Lambda} \right] \quad (12)$$

The above equation can be re-written in the form of the usual RG β -function by including the frequency dependent vertex function into the redefinition of the coupling constant. Then in terms of the logarithmic differential $d\ell = -\frac{d\Lambda}{\Lambda}$, the Eq. 12 can be re-cast into the form:

$$\frac{d\lambda}{d\ell} = -\frac{\lambda}{2} h^2 \quad (13)$$

and finally more compactly expressed in terms of the dimensionless dissipation $\alpha = 2\lambda^2/\Lambda^2$ as

$$\frac{d\alpha}{d\ell} = -\alpha h^2 \quad (14)$$

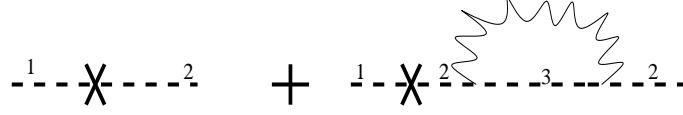


Fig. 5 Diagrams that are involved in the renormalization of the transverse field Δ .

Now, in a similar vein one can calculate the first corrections to the transverse field Δ , with the diagrams depicted in Fig. 5. The technical details of this calculation are very similar to the above calculation, and the final flow equation, written in terms of the scaled magnetic field $h = \Delta/\Lambda$, reads:

$$\frac{dh}{d\ell} = (1 - \alpha)h. \quad (15)$$

The RG equations that we have so far derived are for the case of the ohmic damping. The derivation of the flow equations in the non-ohmic limit is quite straightforward and can be performed by following the technical details elucidated above. Thus, for the sake of brevity we will not perform these computations here. Instead, we will just quote the results of such an exercise. In the presence of non-ohmic dissipation the α flow equation of Eq. 14 gets modified into

$$\frac{d\alpha}{d\ell} = -\alpha h^2 + (1 - s)\alpha. \quad (16)$$

However, the flow of the magnetic field h retains its functional form given in Eq. 15, even in the presence of non-ohmic dissipation.

5 Analyzing the RG flow

In this section we shall discuss the RG flow equations that were derived above. In Sec. 5.1, we shall first analyze the β functions for the ohmic case ($s = 1$). Then, in Sec. 5.2, we shall show that the super-ohmic case ($s > 1$) is bereft of any critical points. Finally in Sec. 5.3, we shall analyze the critical behavior when the bath spectrum is sub-ohmic in character ($0 < s < 1$).

5.1 The RG equations for the ohmic case ($s = 1$)

The situation of the ohmic bath spectrum is probably one of the most well understood case in the study of SBM. This is due to the fact that a linear dispersion of the bath DoS lends itself to an exact mapping to the anisotropic Kondo Model (AKM) [4, 9]. Due to this mapping, it is known that the critical dissipation occurs at $\alpha_c = 1$

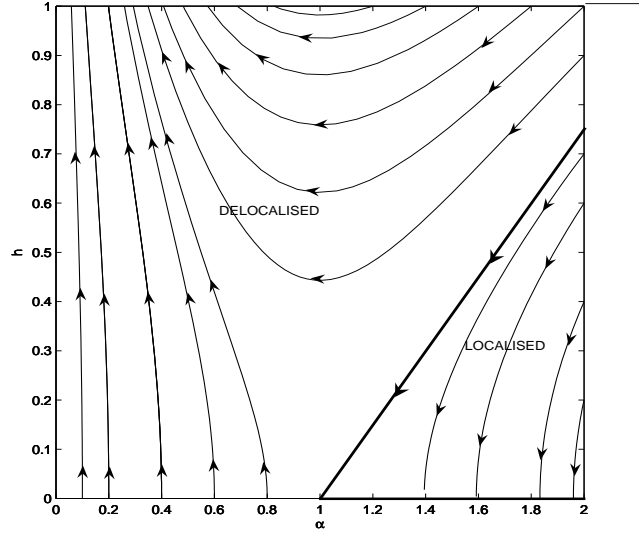


Fig. 6 RG flow for the ohmic SBM ($s = 1$). Here, the flow is constructed numerically by giving various initial (bare) values of the coupling constants h and α . See discussion in Sec. 5.1 for the interpretation.

for small non-zero Δ , and that the phase transition is of the Kosterlitz-Thouless type (infinite order). The flow equations that are found through the mapping to the AKM match the β functions that we obtained by using the Majorana representation (see Eq. 14 and Eq. 15). From the structure of these β functions of the ohmic SBM, it is amply clear that the term $-\alpha h^2$ drives the dissipative coupling to zero whenever $\alpha < 1$. However, in the regime $\alpha > 1$, it is now the transverse field term h that is driven to zero, with the dissipative coupling α renormalizing to a finite value. Furthermore, in the limit $\alpha > 1$ we see that the RG equations, Eq. 14 and Eq. 15, have in fact a line of stable fixed points at zero field, the typical signature of a phase transition of the Kosterlitz-Thouless type. This discussion is encapsulated by Fig. 6, which represents the various RG trajectories that are obtained by numerically solving Eq. 14 and Eq. 15, for various initial values of α and h . From this flow diagram, it is clear that there exists a separatrix such that for any value of α and h that lies below the separatrix, the RG flow terminates at the line of fixed points, whereas if one were to start with initial value of α and h lying above the separatrix, the flow maintains the system in the de-localized phase.

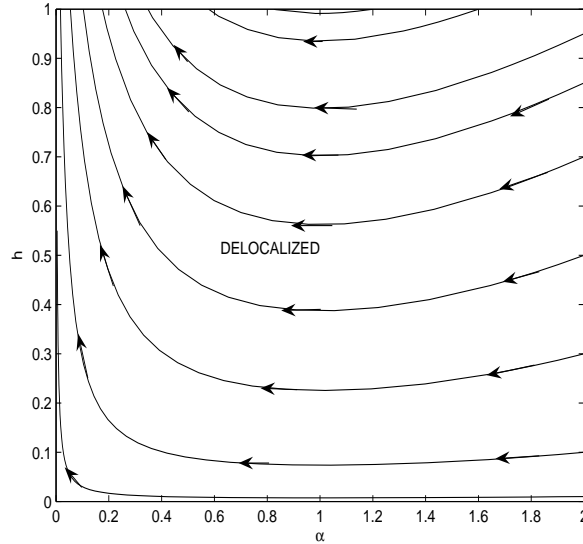


Fig. 7 Flow equations of the super-ohmic SBM model ($s > 1$), starting with various initial values of α and h . For further details refer to Sec. 5.2 in the text.

5.2 The RG equations for the super-ohmic case ($s > 1$)

In the situation where the bath spectrum is super-ohmic, i.e. $s > 1$, it can be readily argued that the system supports no critical fixed points. This fact can be essentially gleaned from solving the set of equations, Eq. 16 and Eq. 15 numerically for various initial configurations of α and h , giving the results depicted in Fig. 7. One sees that for any initial value of the dissipation and the transverse field, the couplings always flow towards the limit $h = \infty$ and $\alpha = 0$. This implies that for the super-ohmic case one always ends up in the de-localized phase, and no quantum phase transition is allowed.

5.3 The RG equations for the sub-ohmic case ($0 < s < 1$)

Now, we turn our attention to the most interesting case, namely the one where the bath spectrum is endowed with a sub-ohmic dispersion, i.e. $0 < s < 1$. Since the mapping of the SBM to the AKM is invalidated in the sub-ohmic regime, the situation of the SBM in the range $0 < s < 1$ was not fully appreciated until recent study from Numerical Renormalization Group (NRG) calculations [2], where a second order quantum phase transition was explicitly demonstrated for all $0 < s < 1$. At this juncture, it should be noted that this localization/delocalization phase tran-

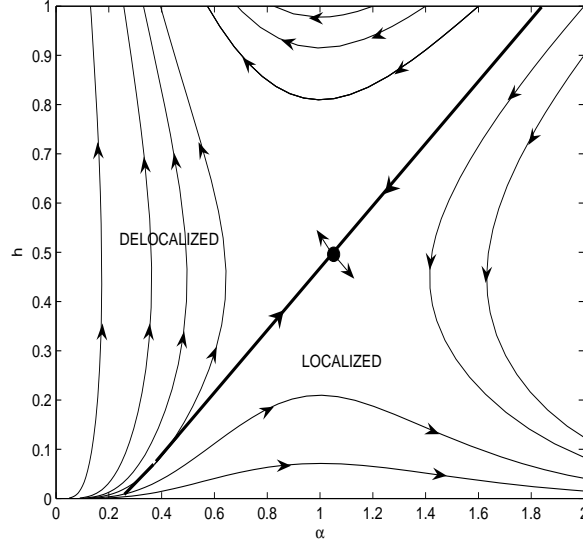


Fig. 8 Flow for the sub-ohmic SBM. Once again, the RG trajectories are plotted for various initial values of the transverse field h and the dissipative coupling α . For further details refer Sec. 5.3 in the text.

sition found in Ref. [2] is missed by the various other analytical treatments of the sub-ohmic SBM, such as variational ansatz or diagonalizations by unitary transformations, but is correctly predicted by the flow equations derived above. The resulting flow is plotted in Fig. 8, with a fixed point occurring at $\alpha_c = 1$ and $h = \sqrt{1-s}$, perturbatively controlled for values of s close to 1.

6 Mapping to a long-ranged Ising Model

In this section, we shall attempt to derive an effective model for the quantum phase transition discussed previously, based purely in terms of the bosonic mode ϕ . This can be done by representing the spin now in terms of Abrikosov fermions [14], and then integrating the fermionic degrees of freedom perturbatively in λ . By using this route we will see that the SBM model can be mapped to a ϕ^4 model with $O(1)$ symmetry and long-ranged interactions in imaginary time. The mapping works as follows:

$$\mathbf{S} = \sum_{\sigma\sigma'} f_{\sigma}^{\dagger} \frac{\sigma_{\sigma\sigma'}}{2} f_{\sigma'} \quad (17)$$

Here, in Eq. 17, the f_{σ}^{\dagger} field are canonical fermions with an imaginary chemical potential [14], that redefines the Matsubara frequencies $\omega_n \rightarrow \omega_n + \pi T/4$, and σ

are the three Pauli matrices. By using Eq. 17 to the defining Hamiltonian of the SBM, (Eq. 2) can be re-written in terms of the following action:

$$S = \int_0^\beta d\tau f^\dagger \left[\partial_\tau - \frac{\Delta}{2} \sigma^x + \frac{\lambda}{2} \sigma^z \sum_i (a_i + a_i^\dagger) \right] f + \int_0^\beta d\tau \sum_i a_i^\dagger (\partial_\tau + \omega_i) a_i. \quad (18)$$

In the above equation f is a two component vector whose Hermitian conjugate is given by $f^\dagger \equiv (f_\uparrow^\dagger, f_\downarrow^\dagger)$. Also in Eq. 18, the ∂_τ term is a consequence of time slicing when going into the path integral representation. The philosophy is now to formally integrate out the fermions to get an perturbative expansion in λ of the effective action. This methodology of integrating out the fermions is very similar in spirit to the treatment by Hertz of the itinerant ferromagnet [7], that we have already alluded to in the introductory section 1. This technical step can be formally performed as the fermionic sector is purely Gaussian, so that the effective theory reads:

$$S_{\text{eff}} = \int_0^\beta d\tau \sum_i a_i^\dagger (\partial_\tau + \omega_i) a_i - \text{Tr} \ln \left[\partial_\tau - \frac{\Delta}{2} \sigma^x + \frac{\lambda}{2} \sigma^z \sum_i (a_i + a_i^\dagger) \right]. \quad (19)$$

Defining the ‘‘local mode’’ $\phi = \sum_i (a_i^\dagger + a_i)$, the bath can be exactly encapsulated by the following Gaussian action, written with the Matsubara frequency $\nu_n = 2n\pi T$:

$$S_{\text{eff}}^{\text{Gauss}} = -\frac{1}{\beta} \sum_{\nu_n} \mathcal{G}_0^{-1}(i\nu_n) \phi(i\nu_n) \phi(-i\nu_n) \quad (20)$$

The quantity \mathcal{G}_0 in the above equation is given by

$$\mathcal{G}_0(i\nu_n) = \sum_i \left(\frac{1}{i\nu_n - \omega_i} + \frac{1}{-i\nu_n - \omega_i} \right) \quad (21)$$

which can be re-expressed in terms of a spectral representation as:

$$\mathcal{G}_0(i\nu_n) = \int d\omega \frac{\rho(\omega)}{i\nu_n - \omega}. \quad (22)$$

Here, in Eq. 22, the bosonic density of states, $\rho(\omega)$ is given by

$$\rho(\omega) = \frac{\omega^s}{\omega_c^{1+s}} \theta(\omega_c + \omega) \theta(\omega_c - \omega) \text{sgn}(\omega). \quad (23)$$

The Green’s function \mathcal{G}_0 can be calculated by substituting the functional form of $\rho(\omega)$ from Eq. 23 into Eq. 22, and then performing the integration over the frequency variable ω . Once we have performed the integration, the resultant expression can be easily inverted to obtain the functional form for \mathcal{G}_0^{-1} which is given in the low frequency limit by

$$\mathcal{G}_0^{-1}(iv_n) = -\frac{s\omega_c}{2} - \left(\frac{s\omega_c}{2}\right)^2 \frac{\pi |v_n|^s}{\sin \frac{\pi s}{2} \omega_c^{s+1}} \quad (24)$$

Thus, substituting the above functional form of the \mathcal{G}_0^{-1} into Eq. 20, we see that the Gaussian part of the action for the bath of harmonic oscillators, Eq. 19, can be written as:

$$S_{\text{eff}}^{\text{Gauss}} = \frac{1}{\beta} \sum_{v_n} \left[\frac{s\omega_c}{2} + \left(\frac{s\omega_c}{2}\right)^2 \frac{\pi |v_n|^s}{\sin \frac{\pi s}{2} \omega_c^{s+1}} \right] |\phi(v_n)|^2 \quad (25)$$

Now, that we have taken care of the Gaussian bath term in Eq. 19, we turn our attention to the $\text{Tr} \ln$ term, which can be Taylor expanded to obtain:

$$\sum_{n=1}^{\infty} \frac{1}{n} \text{Tr} \left(G_0 \sigma^z \phi \frac{\lambda}{2} \right)^{2n}, \quad (26)$$

wherein in the above equation, the quantity G_0 is endowed the functional form, $G_0 = \frac{-i\omega_n \mathbf{1}_2 + \frac{\Delta}{4} \sigma^x}{\omega_n^2 + \frac{\Delta^2}{4}}$, where $\mathbf{1}_2$ is the usual 2×2 identity matrix. Now, we proceed to calculate the traces implicit in Eq. 26. The resultant expression, up to order λ^4 , is then combined with Eq. 25, to obtain:

$$S_{\text{eff}} = \int \frac{d\mathbf{v}}{2\pi} (r + A|\mathbf{v}|^s) |\phi(i\mathbf{v})|^2 + \int d\tau u (\phi(\tau))^4. \quad (27)$$

Here $r = s\omega_c/2 - \lambda^2/(4\Delta)$ is a mass term that controls the distance to criticality, $u = \lambda^4/(16\Delta^3)$ is the leading interaction term, and $A \propto \omega_c^{s-1}$. We note that this action is equivalent to an Ising model in imaginary time, with interaction decaying as $1/(\tau - \tau')^{1+s}$, as expected from the quantum/classical equivalence [5, 2]. Now, one can use simple power-counting arguments to capture the critical behavior of the long-ranged Ising model displayed in Eq. 27, thereby also understanding the critical behavior of the underlying microscopic model, Eq. 2. By doing a power counting analysis around the Gaussian fixed point one finds that the scale dimension of the $O(\phi^4)$ term is $[u] = 2s - 1$. This implies that for all $s < 1/2$ the scale dimension is negative thus implying that the critical behavior is mean field like. However, for $s > 1/2$ one needs to account for higher loop effects to capture the true critical behavior, leading to non trivial exponents with respect to the mean field values.

7 A special identity

In this section, we will derive a special identity that helps us to calculate the fully dressed bosonic propagator in terms of the spin-spin correlator $\chi_z(\tau) = \langle \sigma^z(\tau) \sigma^z(0) \rangle$. We start with an effective action which is a variant of the one that can be obtained from Eq. 2. Thus, we have

$$S[\sigma, \phi, J] = S_{\text{Berry}} - \int d\tau \frac{\Delta}{2} \sigma_z(\tau) + \frac{\lambda}{2} \int d\tau \sigma_x \phi(\tau) + \sum_{\alpha} \int d\tau J^{\alpha}(\tau) \sigma^{\alpha}(\tau) + \int d\tau d\tau' \mathcal{G}_0^{-1}(\tau - \tau') \phi(\tau) \phi(\tau'). \quad (28)$$

Here, in Eq. 28, the term S_{Berry} is the so-called Berry action that encodes the impurity spin commutation relations. This term is not explicitly written down as its functional form relies on spin-coherent states, the discussion of which is beyond the scope of this manuscript. Also, in Eq. 28, J is a source term for the spin dynamics, and \mathcal{G}_0 is again the bare bosonic propagator. The spin-spin correlator can be easily derived from Eq. 28, by performing an appropriate functional differentiation of the partition function Z with respect to the source field J . Thus, we have

$$\chi_z(\tau) = \frac{1}{Z} \frac{\delta^2 Z}{\delta J(\tau) \delta J(0)} \Big|_{J=0} \quad (29)$$

Now, in performing the technical calculations inherent in Eq. 29, one can re-express the bosonic field ϕ in terms of a new field $\tilde{\phi} = \frac{\tau}{\lambda} + \phi$. In doing so we use the fact that the partition function Z remains invariant under such a redefinition of the ϕ field. Thus, re-expressing the partition function in terms of the $\tilde{\phi}$ fields and then performing the functional differentiation, we are led to the following relation that connects $\chi_z(\tau)$ to the full bosonic Green's function $\mathcal{G}_{\phi}(\tau - \tau') = \langle \phi(\tau) \phi(\tau') \rangle$ and the bare bosonic Green's function \mathcal{G}_0 :

$$\chi_z(\tau) = -\frac{4}{\lambda^2} \mathcal{G}_0^{-1}(\tau) + \frac{4}{\lambda^2} \int d\tau_1 d\tau_2 \mathcal{G}_0^{-1}(\tau_1 - \tau) \mathcal{G}_0^{-1}(\tau_2) \langle \phi(\tau_1) \phi(\tau_2) \rangle \quad (30)$$

By going into the frequency domain representation we can compactly re-write Eq. 30 as

$$\chi_z(i\nu_n) = -\frac{4}{\lambda^2} \frac{1}{\mathcal{G}_0(i\nu_n)} + \frac{4}{\lambda^2} \frac{\mathcal{G}_{\phi}(i\nu_n)}{\mathcal{G}_0(i\nu_n)^2} \quad (31)$$

This identity couples the single particle full bosonic propagator \mathcal{G}_{ϕ} to the spin-spin susceptibility χ_z , naively a four operators correlation function (see e.g. the decomposition onto Abrikosov fermions), and shows that both the bosonic field and the longitudinal spin density must become critical altogether at the quantum phase transition. This formula becomes extremely useful in the context of diagrammatic expansions that use the Majorana representation (introduced in section 3), because the spin susceptibility is simply related to the single particle Majorana propagators, leading to a very powerful Ward identity. These further theoretical developments go however much beyond the scope of this review.

However, in the next section, Sec. 8, we shall show the usefulness of the identity derived in this section to recover a well known result in the context of SBM models, the so-called Shiba's relation.

8 Shiba's Relation for the sub-ohmic spin boson model

In this section we establish the Shiba's relation, usually discussed for the ohmic SBM, in the case of the sub-ohmic model $s < 1$. This relation essentially connects the spin correlations at equilibrium to the zero-frequency spin susceptibility (via the free bath spectrum). To derive this we use the fact that the exact bosonic Green's function, on the real frequency axis, has the following low-frequency form (as can be checked by simple perturbative calculations from the effective action Eq. 27)

$$\mathcal{G}_\phi(\nu) = (m + a_s^0 |\nu|^s + i b_s^0 |\nu|^s \text{sgn}(\nu))^{-1} \quad (32)$$

where m is the renormalized mass driving the transition, and a_s, b_s are non critical numerical coefficients. In the limit of small frequencies, the above reduces to:

$$\mathcal{G}_\phi(\nu) = \frac{1}{m} - i \frac{b_s^0}{m^2} |\nu|^s \text{sgn}(\nu) \quad (33)$$

Now, the identity Eq. 31 gives us a relation that connects this full bosonic Green's function \mathcal{G}_ϕ to the spin susceptibility. At low frequency, and introducing the bare mass $m_0 = 1/\mathcal{G}_0(0)$, one obviously gets:

$$\frac{1}{m} = \frac{1}{m_0} - \frac{\lambda^2}{4m_0^2} \chi'_z(0) \quad (34)$$

and

$$\chi''_z(\nu) = -b_s^0 \frac{\lambda^2}{4m_0^2} |\nu|^s \text{sgn}(\nu) [\chi'_z(0)]^2 \quad (35)$$

In Eq. 34 and Eq. 35, the quantities χ'_z and χ''_z are the real and imaginary part of the longitudinal spin susceptibility χ_z . The imaginary part of the bare bosonic Green's function reads: $\mathcal{G}_0''(\nu) = -\frac{J(|\nu|)}{\lambda^2} \text{sgn}(\nu) = -\frac{b_s^0}{m_0^2} |\nu|^s \text{sgn}(\nu)$. Thus, substituting for b_s^0 in Eq. 35, we get:

$$\chi''_z(\nu) = \frac{1}{4} J(|\nu|) \text{sgn}(\nu) [\chi'_z(0)]^2 \quad (36)$$

Finally, from the definition that at $T = 0$ the imaginary part of the spin susceptibility is related to the spin correlation function $C(\nu)$ via the simple relation $\chi''_z = \text{sgn}(\nu)C(\nu)$, we obtain

$$C(\nu) = \frac{1}{4} J(|\nu|) [\chi'_z(0)]^2 \quad (37)$$

which is the generalized Shiba relation for the sub-ohmic spin boson model, and is valid in the low frequency limit for the whole delocalized phase.

9 On the Quantum to Classical mapping

From the general arguments given in the introduction, and the detailed derivation of the classical effective theory Eq. 27 for the specific case of the spin boson model, the results of Ref. [24] came as a surprise, since critical exponents associated to the spin magnetization $\langle S^z \rangle$ were numerically found by these authors to deviate from the expected mean field result for $0 < s < 1/2$. At the time of writing, this issue is still debated [25], see Ref. [6] for a more recent update on the question.

Acknowledgements

RN thanks Priyanka Mohan for generating some of the figures in this manuscript. He also thanks her for discussions and valuable comments.

References

1. D. Belitz, T.R. Kirkpatrick, T. Vojta, Rev. Mod. Phys. **77**, 579 (2005)
2. R. Bulla, N-H Tong and M. Vojta, Phys. Rev. Lett. **91**, 170601 (2003).
3. D. G. Clarke, T. Giamarchi and B. I. Shraiman, Phys. Rev. B **48**, 7070 (1993).
4. T. A. Costi, and G. Zarand, Phys. Rev. B, **59**, 12398, (1999).
5. V. J. Emery and A. Luther, Phys. Rev. B **9**, 215 (1974).
6. S. Florens, A. Freyn, D. Venturelli, and R. Narayanan, unpublished.
7. J. A. Hertz, Phys. Rev. B **14**, 1165 (1976).
8. A. I. Larkin and V. I. Mel'nikov, Sov. Phys. JETP **34**, 656 (1972).
9. A. J. Leggett, S. Chakravarty, A. T. Dorsey, M. P. A. Fisher, A. Garg and W. Zwerger, Rev. Mod. Phys. **59**, 1 (1987).
10. Y. L. Loh, V. Tripathi and M. Turlakov, Phys. Rev. B **71**, 024429 (2005).
11. H. v. Löhneysen, A. Rosch, M. Vojta and P. Wölfle, Rev. Mod. Phys. **79**, 1015 (2007)
12. G. D. Mahan, Many-Particle Physics, Second Edition, Plenum Press, New York, (1990).
13. E. Novais, A. H. Castro Neto, L. Borda, I. Affleck and G. Zarand, Phys. Rev. B **72**, 014417 (2005).
14. V. N. Popov and S. A. Fedotov, Sov. Phys. JETP **67**, 535 (1988).
15. A. M. Sengupta, Phys. Rev. B **61**, 4041 (2000).
16. A. M. Sengupta and A. Georges, Phys. Rev. B **52**, 10295 (1995).
17. Q. Si and J. Llewellyn Smith, Phys. Rev. Lett. **77**, 3339 (1996).
18. M. Vojta, C. Buragohain, and S. Sachdev, Phys. Rev. B **61**, 15152 (2000).
19. D. Venturelli, Masters thesis, un-published.
20. A. J. Millis, Phys. Rev. B **48**, 7183 (1993).
21. W. Mao, P. Coleman, C. Hooley and D. Langreth, Phys. Rev. Lett. **91**, 207203 (2003).
22. A. Shnirman and Y. Makhlin, Phys. Rev. Lett. **91**, 207204 (2003).
23. S. Sachdev, Phys. Rev. B **55**, 142 (1997)
24. M. Vojta, N. Tong, and R. Bulla, Phys. Rev. Lett. **94**, 070604 (2005).
25. A. Winter *et al.*, Phys. Rev. Lett. **102**, 030601 (2009).